Heat stress in tropical highland regions: the case of Kenya during February 2024

G Chagnaud[1,*], J Gacheru[2], C E Birch[3], C M Taylor[1,4]

[1] UK Centre for Ecology and Hydrology, Wallingford, UK

[2] Kenya Meteorological Department, Nairobi, Kenya

[3] School of Earth and Environment, University of Leeds, Leeds, UK

[4] National Centre for Earth Observation, Wallingford, UK

[*] Corresponding author (guicha@ceh.ac.uk)

Abstract

Understanding and awareness about heat stress remain low in sub-Saharan countries despite high exposure and vulnerability. The national media in Kenya reported that people complained about unusual heat stress during February 2024. We combine in-situ and reanalysis data to i) put this event into climatological perspective, and ii) give insights into its surface and atmospheric drivers. Temperature and Heat Index values were 3–4°C above normal during the event; a mid-tropospheric high associated with drier soils contributed to this dry heat stress event. Further research would allow documenting the heat–impacts relationship, needed to improve preparation to future heat extremes.

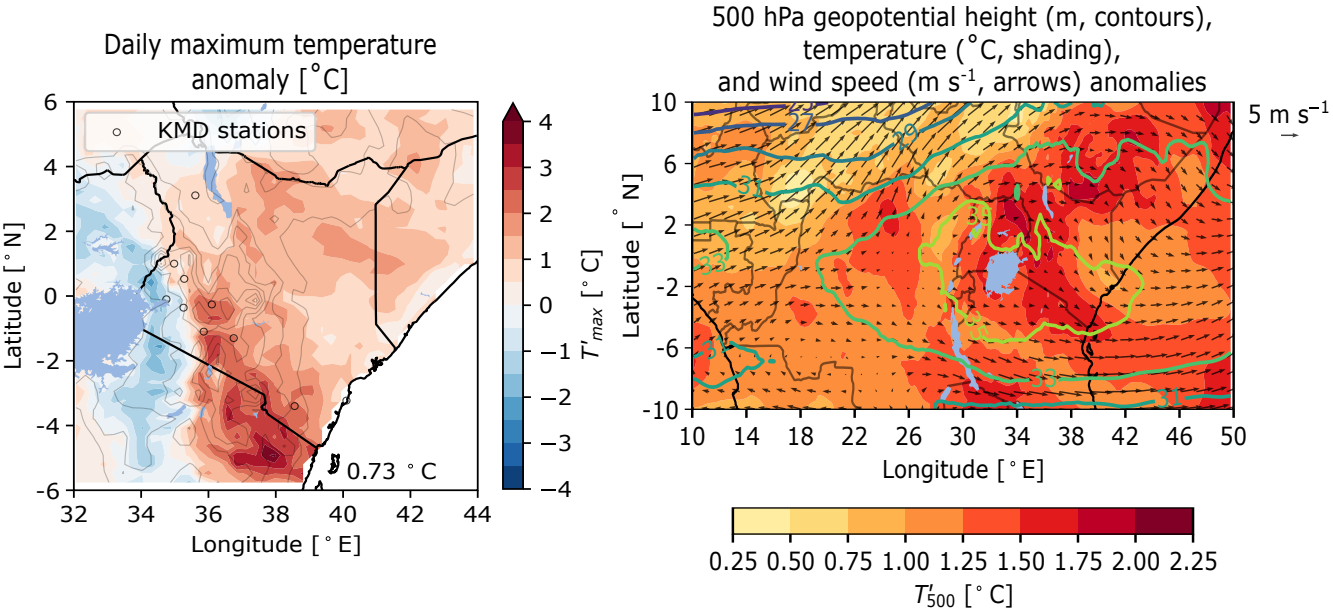

1 Introduction

Heatwaves, which can cause episodes of high heat stress, are considered "silent killers" for two interrelated reasons: first, unlike other extreme weather events such as hurricanes or floods, they leave no physical trace of their passage; second, the effects of heat stress on the human body can build gradually and can have serious consequences including death. These effects often add to pre-existing health conditions, so people in vulnerable groups (older, pregnant, those with chronic illnesses, etc) are affected more (Luber and McGeehin 2008; Ebi et al. 2021; Nunes 2024).

Extreme heat events are among the deadliest weather events; climate change has increased heat-related mortality across many parts of the world (Vicedo-Cabrera et al. 2021) by increasing their frequency, intensity, duration, and areal extent (Matthews et al. 2025). These trends will continue in the future even with moderate greenhouse gases emissions (Gasparrini et al. 2017; Schwingshackl et al. 2021). The impacts of heat stress are numerous, including but not limited to: increased morbidity and mortality, productivity declines in various economic sectors, increased tensions on water, food, electricity, and healthcare. This is especially the case in sub-Saharan Africa, where populations are both exposed given the tropical climate, and vulnerable due to low adaptive capacity and a strong dependence of their economy on outdoor activities. Yet, awareness of the heat–impact relationship, required to mitigate heat risks through relevant adaptation strategies, is still lacking there (Harrington and Otto 2020).

Ambient humidity plays a role in human heat stress through limiting the efficiency of perspiration (e.g., Baldwin et al. 2023). Several heat stress metrics have been developed over the years to provide a more health-relevant measure of the effect of heat on humans than temperature alone (Buzan et al. 2015; Perkins 2015). They all include air temperature and humidity, and some also include solar radiation and wind. Temperature (T) and humidity (specific, q) are weighted differently in these metrics, with two consequences: i) each metric responds differently to a given change in T and q, and ii) the sensitivity to T and q depends on the thermal regime i.e. where we sit in the T–q space at a given location and time. As a result, extreme humid heat values are reached through different mechanisms depending on the time of year, location, and the metric used (Buzan and Huber 2020; Sherwood 2018; Simpson et al. 2023; Ivanovich et al. 2024). Therefore, understanding the causes and impacts of humid heat extremes is challenging.

Another difficulty stems in the definition of thresholds for which health impacts of humid heat are expected and/or reported. For instance, the wet-bulb temperature (Twb) value of 35°C has long been considered an upper limit to human survivability (Sherwood and Huber 2010), based solely on thermodynamical considerations. However, physiological studies have reported serious impacts at Twb values above 24–27°C, depending on personal factors such as age and health condition, as well as on exertion and clothing (Vecellio et al. 2022). Furthermore, not only survivability matters but also liveability. In this regard, Vanos et al. (2023) found that "young adults reach a limit in their ability to perform any activity safely" at relative humidity of 75 % and temperatures above 35.5°C (i.e. Twb $\geq$ 31.5°C at 1000 hPa). For the Heat Index (HI), the US national weather services (NWS) has defined the Caution (HI $\in$ [27, 32°C]), Extreme Caution ([33, 39°C]), Danger ([40, 51°C]), and Extreme Danger (HI $\geq$ 52°C) categories, each with its associated effects on the human body[1]. In short, the heat-health relationship is highly multi-dimensional and context-dependent; an array of approaches, from individual-scale physiological experiments

[1] See `https://www.weather.gov/ama/heatindex`

to large-scale epidemio-meteorological studies are needed to improve our understanding of this relationship.

Our case study analysis was motivated by national and social media reports of people complaining about unusually high heat during February 2024 in Kenya [2, 3]. This was especially the case between 15$^{\text{th}}$ and 20$^{\text{th}}$ February 2024 in the highlands of Kenya, one of the most densely populated region in this part of East Africa that also includes the capital of Kenya, Nairobi (Fig.1a).

The seasonal cycle of rainfall in East Africa shows that February precedes the start of the long rainy season (Fig.1b). February is the second warmest month for average temperature and the first in terms of peak daily temperatures; it is also among the driest months (Fig.1b). The highlands have a cooler and drier climate compared to the rest of the country, as shown in Fig.1c and d, respectively. This is largely the result of topography, with lower temperatures (15–20°C) in the highlands than in the rest of the region. The Indian Ocean also influences the hydroclimate of Kenya, with cooler/more humid conditions near the coast and warmer/drier conditions further inland.

The analysis of observed trends in February means of daily minimum and daily maximum temperatures (T_{min} and T_{max}, respectively) shows that on average, T_{min} is increasing at 0.6°C per decade since 1995, with eight stations recording a significant positive trend (Fig.1e). Interestingly, the largest T_{min} trends, of ≈ 1°C dec.$^{-1}$, are located in the highlands. In contrast, T_{max} is stable over the 1995–2024 period, with none of the seven increasing trends nor the three decreasing trends passing the 5 % level significance test (Fig.1f).

In this context, we seek to characterize the 15–20$^{\text{th}}$ February 2024 event from a climatological perspective, and to gain insights into its meteorological drivers. We focus our analysis on the wet-bulb temperature and the Heat Index, whose definitions rely on T and q only.

[2] https://citizen.digital/news/its-unbearable-kenyans-concerned-as-nairobi-gets-too-hot-n336997

[3] https://theconversation.com/kenyas-had-unusually-hot-weather-an-expert-unpacks-what-could-be-causing-it-224348

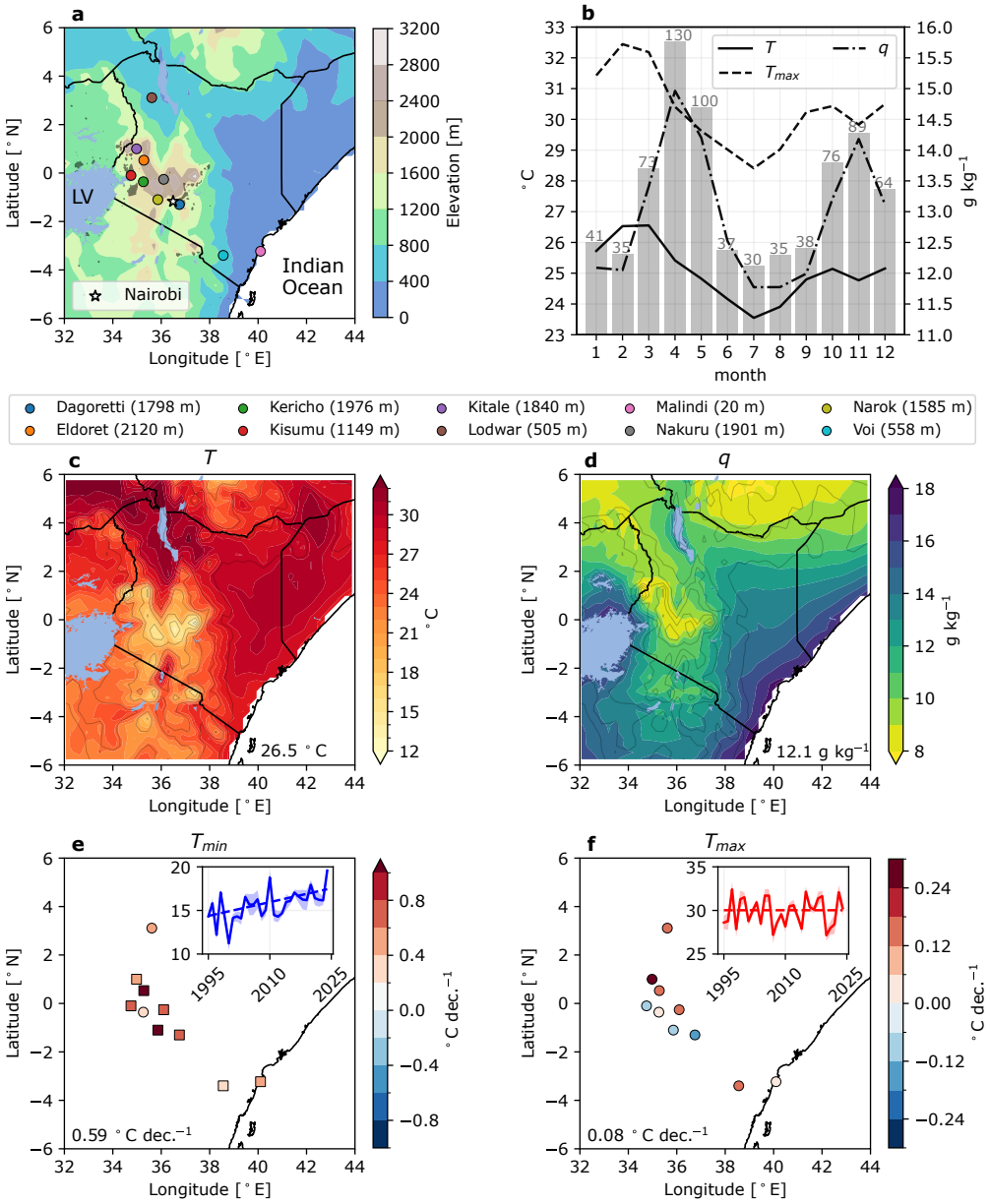

Figure 1: (a) Terrain elevation (shading, in meters) and population density (areas with a population density ≥ 500 inhabitants km^{-2} are shaded in black). The location of the Kenya Meteorological Department (KMD) stations used in this study are indicated with dots (station names in the legend below). The star denotes Nairoba and "LV" stands for Lake Victoria. (b) 1995–2024 monthly averages of daily mean temperature (solid line), daily maximum temperature (dashed line), specific humidity (dashed-dotted line), and 2001–2022 mean monthly cumulative rainfall (bars; values indicated on top of each bar, in mm). February mean (c) temperature and (d) specific humidity; the numbers in the bottom right corner of each panel are the spatial averages. 1995–2024 trends in February mean (e) T_{min} and (f) T_{max} estimated with a Theil-Sen slope at each KMD station. Trends significant at the 5 % level (p-value ≤ 0.05) according to a Mann-Kendall test are depicted with squares. Insets show the time series of regional T_{min} and T_{max} for February. The shading about the lines denotes $\pm$ 1 standard deviation across stations. The dashed lines are the Theil-Sen trend estimates.

2 Data and Methods

Daily rainfall data from the Integrated Multi-satellitE Retrievals for GPM (GPM-IMERG, Huffman et al. 2015) for 2001–2022 are used to compute the mean seasonal cycle of rainfall in the study domain (6°S–6°N, 32–44°E). Temperature data extracted from manned weather station records are used to compute trends in monthly means of daily minimum and daily maximum temperatures using a Theil-Sen's slope estimation (Sen 1968). The significance of trends is assessed with the Mann-Kendall test (Mann 1945). Hourly dry-bulb temperature, dewpoint temperature, and surface pressure provided by automatic weather stations since 2023 are used to compute hourly Twb values with R. Warren and C. Raymond's Python implementation[4] of the Davies-Jones formula (Davies-Jones 2008). Hourly HI values are calculated from dry-bulb temperature and relative humidity based on the Rothfusz regression (after Steadman 1979), following the US NWS guidance[5] and with corrections from Romps and Lu (2022). Data from the ERA5 reanalysis (Hersbach et al. 2020) are used to compute the regional mean seasonal cycles of daily mean temperature, daily mean specific humidity, and daily maximum temperature (Fig.1b). Because the available hourly in situ data do not allow for a long-term analysis, ERA5 data are also used to compute daily anomalies in humid heat metrics during 15–20$^{\text{th}}$ February 2024 with respect to their 1995–2024 climatology: anomalies of daily maximum T (T'_{max}), HI (HI'$_{max}$), and Twb (Twb'$_{max}$) are computed separately for each calendar day by subtracting the value for that day to the corresponding 1995–2024 mean, before taking the week average. The significance of the anomalies is assessed with a Mann-Whitney test (Mann and Whitney 1947).

3 Results

Figures 2a and 2b show, for each highland station, T and q at the time of daily maxima of HI and Twb, respectively, for each day of 15–20$^{\text{th}}$ February 2024 (dots) and averaged across the month (squares). On top of T and q values are plotted isolines of HI, Twb, and relative humidity (RH). All daily maxima of HI have T above 25°C and RH between 20 % and 60 %. In contrast, observations sampled at the time of daily Twb maxima are associated with cooler and moister (in both absolute and relative terms) environments.

Almost all daily maxima of HI recorded during 15–20$^{\text{th}}$ February 2024 are located to the right of the HI isoline that crosses their corresponding monthly mean values (Fig.2a). In contrast, daily maxima of Twb are scattered on either side of the Twb isoline (Fig.2b). Hence, anomalies in humid heat values during 15–20$^{\text{th}}$ Feb 2024 (compared to the month average) were larger for HI than for Twb, meaning that the Heat Index seems more appropriate for assessing the heat stress experienced by the population during this particular episode. It can also be noted in Figures 2a and 2b that below about T=27°C, isolines of HI are almost vertical i.e. parallel to isolines of T. Therefore, in this region of the T–q space, a departure from the HI climatology is more likely to result from a larger increase in T (shift to the right) relative to an increase in q (shift upward). In fact, most dots in Fig.2a are associated with a clear increase in T, whereas changes in q have little effect on HI. Beyond these essentially qualitative considerations, it should be noted that several daily maxima of HI recorded during the week belong to the Caution category (HI $\in$ [27–32°C]), for which effects on health (e.g., fatigue) begin to occur.

[4]Available at `https://github.com/cr2630git/wetbulb_dj08_spedup`

[5]Available at `https://www.wpc.ncep.noaa.gov/html/heatindex_equation.shtml`

The consequences of heat stress also depend on how unusual it is at a particular time of year and location. We therefore evaluate how daily maxima of T, HI, and Twb that occurred during 15–20$^{\text{th}}$ February 2024 compare with typical values for this time of year (see Data and Methods). Figure 2c shows that, on average during the event, T'_{max} is up to 4°C above normal over the eastern highlands. In contrast, negative values are founds around Lake Victoria. The HI'$_{max}$ pattern broadly resembles this, with some localised maxima 2–3°C above normal (Fig.2d). The surroundings of Lake Victoria are also cooler than usual although to a lesser extent than for T'_{max}. Twb'$_{max}$ shows a somewhat opposite pattern, with positive anomalies of 2–3°C in the westernmost part of Kenya and of ≈1°C over the highlands. This confirms that the heat perceived by the population in the highlands was mainly driven by an increase in T, with changes in q having distinct modulating effects on HI and Twb. We next analyse the meteorological drivers of this event by comparing atmospheric and surface variable values during the week 15–20$^{\text{th}}$ February 2024 with their climatology.

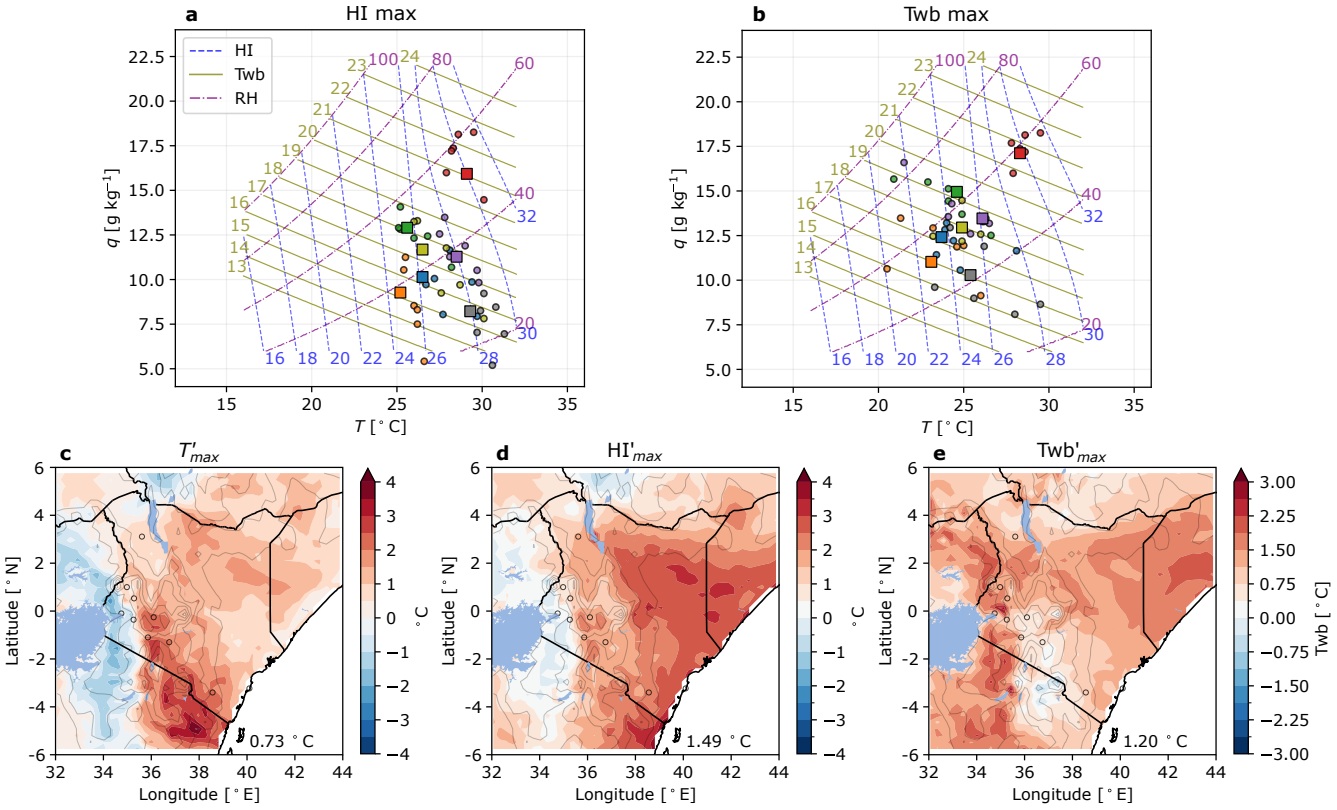

Figure 2: Joint distribution of T (in °C; x-axis) and q (in g kg^{-1}; y-axis) sampled at the time of daily maximum (a) HI and (b) Twb, at each highland station (color code similar to Fig.1a). Squares denote the median of the marginal distributions of T and q across all days of February 2024. Dots denote the days between 15$^{\text{th}}$ and 20$^{\text{th}}$ February 2024. Isolines of HI, Twb, and relative humidity (RH) are shown with blue dashed, olive solid, and purple dotted-dashed lines, respectively. 15–20$^{\text{th}}$ February 2024 averages in anomalies of daily maximum (c) T, (d) HI, and (e) Twb (note the different color scale for this latter). Orography is denoted with gray contours (see Fig.1a for elevation values).

The heat event of February 2024 occurs in the aftermath of the third largest El Nino Southern Oscillation

(ENSO) episode since 1995, peaking at +2°C in November 2023 (Fig.3a). ENSO generates warm air temperature anomalies across the Tropics (e.g., Soden 2000), with tropospheric temperature anomalies generally lagging ENSO by a few months (Sobel et al. 2002, see Fig.3a). Figure 3b shows that the mid-troposphere was warmer than usual for this time of year, with air temperature at 500 hPa 1.25 to 2.25°C above the long-term average from southwestern Kenya to southern Ethiopia. These warm anomalies are associated with a high pressure system centered above Lake Victoria, with 500 hPa geopotential height anomalies (z'_{500}) larger than 35 meters. This high pressure system has a divergent circulation on its Northern and Southern edges; associated with this, subsidence may have favoured clear-sky conditions and increased solar radiation. A similar situation is seen closer to the surface: air temperature at 850 hPa is 1.5 to 3°C above climatology in southern Kenya; the largest geopotential height anomalies, of 10–20 m, are centered on Lake Victoria; and there are easterly anomalies of 3–4 m s^{-1} on either side of the Lake (Fig.3c). However, air temperature is slightly cooler than usual around Lake Victoria, likely reflecting the influence of surface conditions (due to topography, the 850 hPa geopotential height, z_{850}, is close to the surface in this area). Near-surface air temperature anomalies resemble well their 850 hPa counterpart (Fig.3d): T' values of 2–3°C are found in large parts of Kenya, except around Lake Victoria and further South, where T' values of ≈-1°C are found. This confirms that anomalously warm air has contributed substantially to enhancing HI and to lesser extent, Twb (Fig.2d and e, respectively).

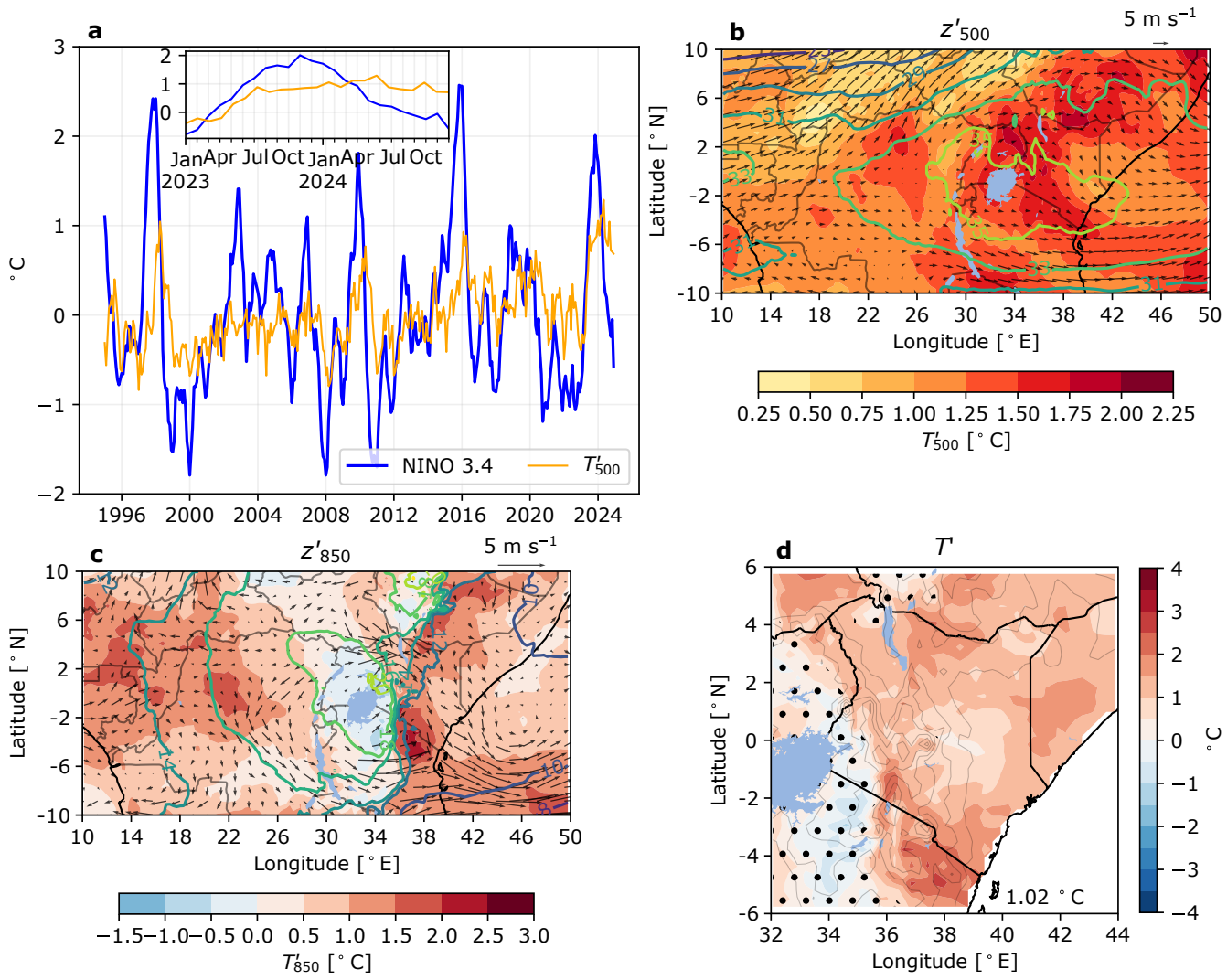

Figure 3: (a) 1995-2024 time series of the monthly El-Nino Southern Oscillation 3.4 index (NINO 3.4, blue line) and the pan-Tropical (30°S−30°N, 180°W−180°E) monthly mean temperature anomaly at 500 hPa (T'_{500}, orange line) with respect to the 1995–2024 average. The inset shows the 2023–2024 period. 15–20$^{\text{th}}$ February 2024 daily anomaly averages of (b) geopotential height (contours, in m), temperature (shading, in °C) and total wind speed (vectors, in m s^{-1}) at 500 hPa. (c) Same as (b) but at 850 hPa. (d) 15–20$^{\text{th}}$ February 2024 daily anomaly averages of near-surface temperature (T'); the domain-average anomaly is indicated in the bottom right corner; anomalies significant at the 5 % level are *not* stippled; orography is denoted with gray contours (see Fig.1a for elevation values).

We next examine whether the land surface conditions have also played a role in modulating humid heat during the sequence of days. Figure 4a shows that top layer (0–7 cm) soil moisture anomalies within -2 to -6 mm are found over the highlands. Solar radiation hitting drier soils may be preferentially converted into sensible heat flux. Sensible heat flux anomalies of 25–50 W m^{-2}, found in areas of negative soil moisture anomalies (Fig.4b), contribute to enhanced warming of the near-surface air. For reference, a perfectly isolated air volume with a surface of 1 km×1 km and a height of 1 km (typically the average depth of the planetary boundary layer) would warm up by ≈0.9°C

with a heat flux of 25 W m^{-2} imposed for 12 hours. Figure 4a also shows areas of positive soil moisture anomalies to the East and South of Lake Victoria, resulting in solar radiation being preferentially converted into latent heat flux there, as shown in Figure 4c. Enhanced evaporation over wet soils moistens the near-surface air, resulting in specific humidity anomalies of 2.5–3.5 g kg^{-1} (Fig.4d). These latter explain why positive daily maximum Twb anomalies were found there (Fig.2e), having in mind that Twb is more sensitive to changes in q than to changes in T (Sherwood 2018).

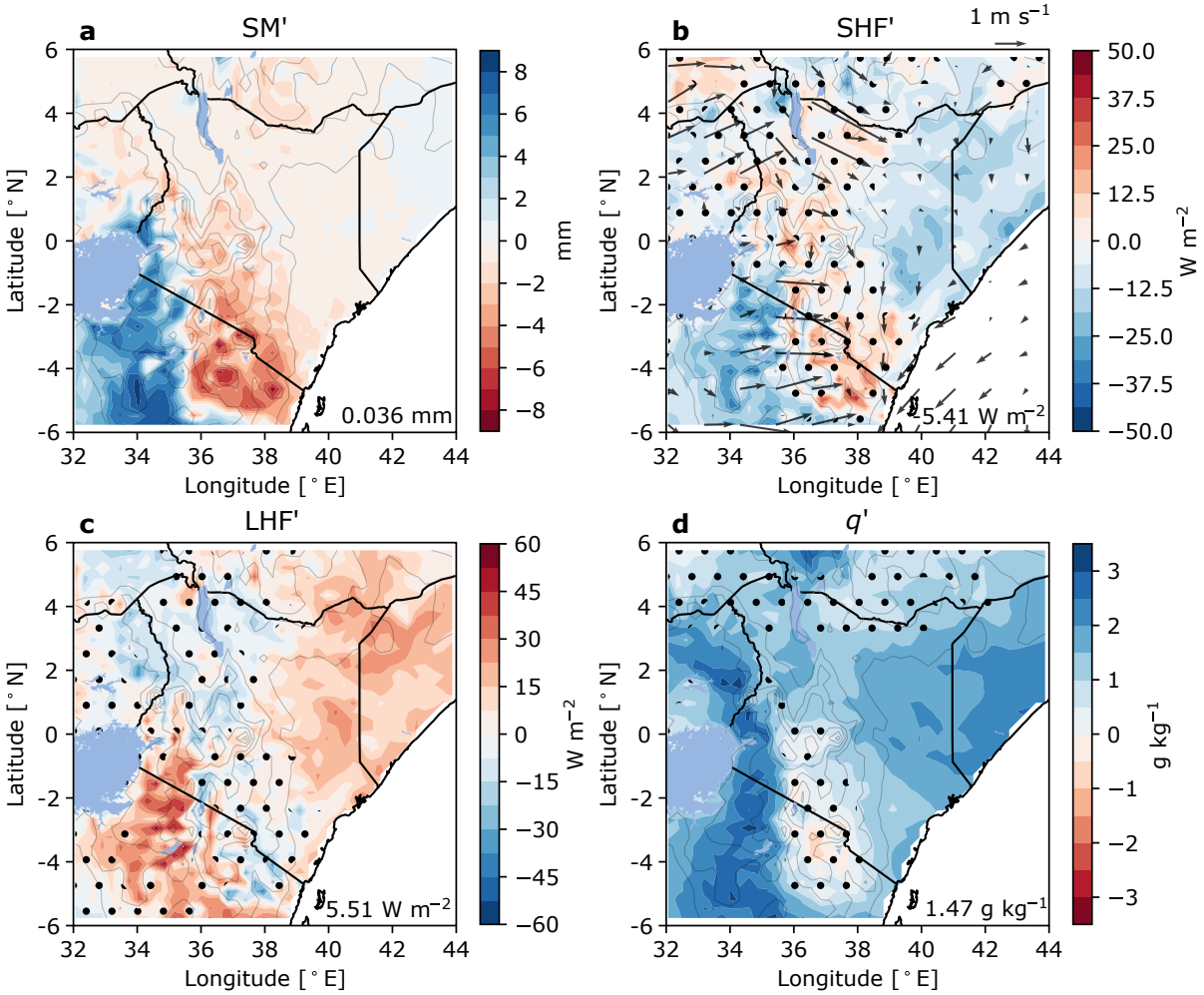

Figure 4: 15–20$^{\text{th}}$ February 2024 daily anomaly averages of (a) top layer soil moisture (SM'), (b) sensible heat flux (SHF'), (c) latent heat flux (LHF'), and (d) specific humidity (q'); 10-meter wind speed anomalies are also displayed with arrows in (b). The domain-average anomaly for each variable is indicated in the bottom right corner of each panel. Anomalies significant at the 5 % level are *not* stippled, except for SM' where it is the opposite. Orography is denoted with gray contours (see Fig.1a for elevation values).

4 Discussion and conclusion

This analysis of a heat event from the perspective of two humid heat metrics allows us to infer which metric best captures the heat perceived by the population. It was found that the heat perceived by the inhabitants of

the Kenyan highlands during 15–20$^{\text{th}}$ February 2024 was largely dry in nature, with daily maxima of dry-bulb temperature 3–4°C above normal whereas specific humidity was reduced by 0.5–1 g kg^{-1}. As a result, daily maxima of the Heat Index were enhanced by 2–3°C, whereas daily maxima of the more q-sensitive wet-bulb temperature were ≈0.5°C below normal for that time of year. In addition, some HI values recorded during the were close to or within the Caution category, for which health impacts can occur; in contrast, Twb values were below known physiological thresholds. This event resulted from a favourable situation at the synoptic-scale, with mid-tropospheric temperatures 1.25 to 2.25°C above normal following the strong ENSO state that prevailed in the previous months. Furthermore, anormally high near-surface temperatures were likely amplified by the warming of air through sensible heat flux enhancement at the expense of surface evaporation over drier soils; this "upward" land-atmosphere coupling mechanism is known to amplify dry heatwaves (e.g., Seneviratne et al. 2006; Miralles et al. 2014).

This study contributes to documenting the meteorological drivers of heat hazards in a tropical highland region by considering the modulating and often over-looked role of humidity, and by providing insights on the underlying mechanisms. In this respect, an obvious next step would be to carry out a systematic process-based analysis of dry and humid heat extremes in East Africa, which remains a critical gap in the scientific literature. It should also be noted that Twb and HI may only partially reflect the heat stress experienced by the population, as neither of these metrics consider the role of radiation and wind on human thermoregulation. In fact, anticyclonic conditions are generally associated with clear sky and weak near-surface wind, which would result in larger solar radiation and lower sweat evaporation rates, respectively. It can therefore be expected that heat stress metrics that include one or both variables –such as the wet-bulb globe temperature and the universal thermal comfort index– will display even larger anomalies. On that note, Kong et al. (2025) show that inter-metrics spread in heat stress change over the past 4 decades is primarily driven by differences in temperature-humidity relative weight, suggesting that metrics embedding only these two variables may be sufficient to assess future heat stress trends.

This study was prompted by media reports and is therefore limited in scope. Yet, heat hazards are ubiquitous and their health consequences can remain under the radar, sometimes settling in for the long term (Nunes 2024). Improving our understanding of the heat–health relationship thus requires systematic surveys that monitor the multifaceted effects of heat stress on humans, spanning the diversity of climatological, physiological, and socioeconomic contexts.

In addition to its effect on health, severe heat can affect a variety of socioeconomic sectors such as agriculture (crops, livestock) and energy (power generation systems). Notwithstanding the fact that quantifying critical thresholds for all the different potential heat impacts remains difficult, these impacts can have high economic costs in sub-Saharan Africa (Burke et al. 2015; Parkes et al. 2019). Raising awareness and preparing individuals, communities, as well as local and national institutions in sub-Saharan countries, for heat-related risks is therefore crucial under unabated global warming. This study is part of a wider collaboration between the Kenya Meteorological Department and UK-based researchers, aiming at improving heat risk monitoring and forecasting at KMD and across East Africa. KMD has recently implemented humid heat forecasts in their weekly county-level weather bulletins[6]. Future work will be dedicated to the development of an early warning system for heat, combining land

[6] `https://meteo.go.ke/our-products/county-forecasts/`

surface observations and numerical weather model outputs to predict humid heat hours to days in advance. Heat hazard alerts will be communicated to the last-mile users, including vulnerable populations such as farmers and outdoor workers, via KMD's dissemination channels (SMS, local radio, TV).

Acknowledgment

The authors thank Joshua Talib for initiating this collaboration with KMD and are grateful to KMD staff for the provision and preparation of meteorological data. This work was supported by the Natural Environment Research Council as part of the NC for Global Challenges programme [NE/X006247/1] delivering National Capability.

Conflict of interests

The authors declare no conflict of interest.

Data availability

In situ data are the property of the Kenyan Meteorological Department and are not freely available. GPM-IMERG data are available at `https://disc.gsfc.nasa.gov/datasets/GPM_3IMERGDF_07/summary`. ERA5 data are available from the Copernicus Climate Change Service (C3S) Climate Data Store (CDS) at Hersbach et al. (2023). Population density data were extracted from `https://www.earthdata.nasa.gov/data/projects/gpw`.

References

Baldwin, Jane W., Benmarhnia, Tarik, Ebi, Kristie L., Jay, Ollie, Lutsko, Nicholas J., and Vanos, Jennifer K. (2023). "Humidity's Role in Heat-Related Health Outcomes: A Heated Debate". en. In: *Environmental Health Perspectives* 131.5, p. 055001.

Burke, Marshall, Hsiang, Solomon M., and Miguel, Edward (2015). "Global non-linear effect of temperature on economic production". en. In: *Nature* 527.7577, pp. 235–239.

Buzan, J R, Oleson, K, and Huber, M (2015). "Implementation and comparison of a suite of heat stress metrics within the Community Land Model version 4.5". en. In: *Geosci. Model Dev.*

Buzan, Jonathan R and Huber, Matthew (2020). "Moist Heat Stress on a Hotter Earth". en. In.

Davies-Jones, Robert (2008). "An Efficient and Accurate Method for Computing the Wet-Bulb Temperature along Pseudoadiabats". en. In: *Monthly Weather Review* 136.7, pp. 2764–2785.

Ebi, Kristie L, Capon, Anthony, Berry, Peter, Broderick, Carolyn, De Dear, Richard, Havenith, George, Honda, Yasushi, Kovats, R Sari, Ma, Wei, Malik, Arunima, Morris, Nathan B, Nybo, Lars, Seneviratne, Sonia I, Vanos, Jennifer, and Jay, Ollie (2021). "Hot weather and heat extremes: health risks". en. In: *The Lancet* 398.10301, pp. 698–708.

Gasparrini, Antonio, Guo, Yuming, Sera, Francesco, Vicedo-Cabrera, Ana Maria, Huber, Veronika, Tong, Shilu, De Sousa Zanotti Stagliorio Coelho, Micheline, Nascimento Saldiva, Paulo Hilario, Lavigne, Eric, Matus Correa, Patricia, Valdes Ortega, Nicolas, Kan, Haidong, Osorio, Samuel, Kyselý, Jan, Urban, Aleš, Jaakkola, Jouni J K, Ryti, Niilo R I, Pascal, Mathilde, Goodman, Patrick G, Zeka, Ariana, Michelozzi, Paola, Scortichini, Matteo, Hashizume, Masahiro, Honda, Yasushi, Hurtado-Diaz, Magali, Cesar Cruz, Julio, Seposo, Xerxes, Kim, Ho, Tobias, Aurelio, Iñiguez, Carmen, Forsberg, Bertil, Åström, Daniel Oudin, Ragettli, Martina S, Guo, Yue Leon, Wu, Chang-fu, Zanobetti, Antonella, Schwartz, Joel, Bell, Michelle L, Dang, Tran Ngoc, Van, Dung Do, Heaviside, Clare, Vardoulakis, Sotiris, Hajat, Shakoor, Haines, Andy, and Armstrong, Ben (2017). "Projections of temperature-related excess mortality under climate change scenarios". en. In: *The Lancet Planetary Health* 1.9, e360–e367.

Harrington, Luke J. and Otto, Friederike E. L. (2020). "Reconciling theory with the reality of African heatwaves". en. In: *Nature Climate Change* 10.9. Publisher: Nature Publishing Group, pp. 796–798.

Hersbach, H, Bell, B, Berrisford, P, Biavati, G, Horányi, A, Muñoz Sabater, J, Nicolas, J, Peubey, C, Radu, R, Rozum, I, Schepers, D, Simmons, A, Soci, C, Dee, D, and Thépaut, J-N (2023). "ERA5 hourly data on single levels from 1940 to present". [Dataset]. In: *Copernicus Climate Change Service (C3S) Climate Data Store (CDS)*.

Hersbach, Hans, Bell, Bill, Berrisford, Paul, Hirahara, Shoji, Horányi, András, Muñoz-Sabater, Joaquín, Nicolas, Julien, Peubey, Carole, Radu, Raluca, and Schepers, Dinand (2020). "The ERA5 global reanalysis". In: *Quarterly Journal of the Royal Meteorological Society* 146.730, pp. 1999–2049.

Huffman, George J, Bolvin, David T, Braithwaite, Dan, Hsu, Kuolin, Joyce, Robert, Xie, Pingping, and Yoo, Soo-Hyun (2015). "NASA global precipitation measurement (GPM) integrated multi-satellite retrievals for GPM (IMERG)". In: *Algorithm theoretical basis document (ATBD) version* 4.26, p. 30.

Ivanovich, Catherine C., Sobel, Adam H., Horton, Radley M., and Raymond, Colin (2024). "Stickiness: A New Variable to Characterize the Temperature and Humidity Contributions toward Humid Heat". en. In: *Journal of the Atmospheric Sciences* 81.5, pp. 819–837.

Kong, Qinqin, Jing, Renzhi, Raymond, Colin, Tuholske, Cascade, Heft-Neal, Sam, Wagner, Zachary, Wang, Zetianyu, Zimmer, Andrew, Huber, Matthew, and Bendavid, Eran (2025). *Spatial patterns of historical changes in human heat stress disagree across metrics*. en.

Luber, George and McGeehin, Michael (2008). "Climate Change and Extreme Heat Events". en. In: *American Journal of Preventive Medicine* 35.5, pp. 429–435.

Mann, H. B. and Whitney, D. R. (1947). "On a Test of Whether one of Two Random Variables is Stochastically Larger than the Other". In: *The Annals of Mathematical Statistics* 18.1. Publisher: Institute of Mathematical Statistics, pp. 50–60.

Mann, Henry B. (1945). "Nonparametric Tests Against Trend". In: *Econometrica* 13.3. Publisher: [Wiley, Econometric Society], pp. 245–259.

Matthews, Tom, Raymond, Colin, Foster, Josh, Baldwin, Jane W., Ivanovich, Catherine, Kong, Qinqin, Kinney, Patrick, and Horton, Radley M. (2025). "Mortality impacts of the most extreme heat events". en. In: *Nature Reviews Earth & Environment* 6.3, pp. 193–210.

Miralles, Diego G., Teuling, Adriaan J., Van Heerwaarden, Chiel C., and Vilà-Guerau De Arellano, Jordi (2014). "Mega-heatwave temperatures due to combined soil desiccation and atmospheric heat accumulation". en. In: *Nature Geoscience* 7.5, pp. 345–349.

Nunes, Ana Raquel (2024). "Heatwaves: The Silent Killers of Public Health". en. In: *Disaster Medicine and Public Health Preparedness* 18, e227.

Parkes, Ben, Cronin, Jennifer, Dessens, Olivier, and Sultan, Benjamin (2019). "Climate change in Africa: costs of mitigating heat stress". en. In: *Climatic Change* 154.3-4, pp. 461–476.

Perkins, Sarah E. (2015). "A review on the scientific understanding of heatwaves—Their measurement, driving mechanisms, and changes at the global scale". In: *Atmospheric Research* 164-165, pp. 242–267.

Romps, David M and Lu, Yi-Chuan (2022). "Chronically underestimated: a reassessment of US heat waves using the extended heat index". en. In: *Environmental Research Letters* 17.9. Publisher: IOP Publishing, p. 094017.

Schwingshackl, Clemens, Sillmann, Jana, Vicedo-Cabrera, Ana Maria, Sandstad, Marit, and Aunan, Kristin (2021). "Heat Stress Indicators in CMIP6: Estimating Future Trends and Exceedances of Impact-Relevant Thresholds". en. In: *Earth's Future* 9.3, e2020EF001885.

Sen, Pranab Kumar (1968). "Estimates of the Regression Coefficient Based on Kendall's Tau". In: *Journal of the American Statistical Association* 63.324. Publisher: ASA Website _eprint: https://www.tandfonline.com/doi/pdf/10.1080/01621459.1968.10480934 pp. 1379–1389.

Seneviratne, Sonia I., Lüthi, Daniel, Litschi, Michael, and Schär, Christoph (2006). "Land–atmosphere coupling and climate change in Europe". en. In: *Nature* 443.7108, pp. 205–209.

Sherwood, Steven C. (2018). "How Important Is Humidity in Heat Stress?" en. In: *Journal of Geophysical Research: Atmospheres* 123.21.

Sherwood, Steven C. and Huber, Matthew (2010). "An adaptability limit to climate change due to heat stress". en. In: *Proceedings of the National Academy of Sciences* 107.21, pp. 9552–9555.

Simpson, Charles H., Brousse, Oscar, Ebi, Kristie L., and Heaviside, Clare (2023). "Commonly used indices disagree about the effect of moisture on heat stress". en. In: *npj Climate and Atmospheric Science* 6.1, p. 78.

Sobel, Adam H., Held, Isaac M., and Bretherton, Christopher S. (2002). "The ENSO Signal in Tropical Tropospheric Temperature". EN. In: *Journal of Climate* 15.18. Publisher: American Meteorological Society Section: Journal of Climate, pp. 2702–2706.

Soden, Brian J. (2000). "The Sensitivity of the Tropical Hydrological Cycle to ENSO". EN. In: *Journal of Climate* 13.3. Publisher: American Meteorological Society Section: Journal of Climate, pp. 538–549.

Steadman, R. G. (1979). "The Assessment of Sultriness. Part I: A Temperature-Humidity Index Based on Human Physiology and Clothing Science". EN. In: *Journal of Applied Meteorology and Climatology* 18.7. Publisher: American Meteorological Society Section: Journal of Applied Meteorology and Climatology, pp. 861–873.

Vanos, Jennifer, Guzman-Echavarria, Gisel, Baldwin, Jane W., Bongers, Coen, Ebi, Kristie L., and Jay, Ollie (2023). "A physiological approach for assessing human survivability and liveability to heat in a changing climate". en. In: *Nature Communications* 14.1, p. 7653.

Vecellio, Daniel J., Wolf, S. Tony, Cottle, Rachel M., and Kenney, W. Larry (2022). "Evaluating the 35°C wet-bulb temperature adaptability threshold for young, healthy subjects (PSU HEAT Project)". In: *Journal of Applied Physiology* 132.2. Publisher: American Physiological Society, pp. 340–345.

Vicedo-Cabrera, A. M., Scovronick, N., Sera, F., Royé, D., Schneider, R., Tobias, A., Astrom, C., Guo, Y., Honda, Y., Hondula, D. M., Abrutzky, R., Tong, S., Coelho, M. De Sousa Zanotti Stagliorio, Saldiva, P. H. Nascimento, Lavigne, E., Correa, P. Matus, Ortega, N. Valdes, Kan, H., Osorio, S., Kyselý, J., Urban, A., Orru, H., Indermitte, E., Jaakkola, J. J. K., Ryti, N., Pascal, M., Schneider, A., Katsouyanni, K., Samoli, E., Mayvaneh, F., Entezari, A., Goodman, P., Zeka, A., Michelozzi, P., de'Donato, F., Hashizume, M., Alahmad, B., Diaz, M. Hurtado, Valencia, C. De La Cruz, Overcenco, A., Houthuijs, D., Ameling, C., Rao, S., Di Ruscio, F., Carrasco-Escobar, G., Seposo, X., Silva, S., Madureira, J., Holobaca, I. H., Fratianni, S., Acquaotta, F., Kim, H., Lee, W., Iniguez, C., Forsberg, B., Ragettli, M. S., Guo, Y. L. L., Chen,

B. Y., Li, S., Armstrong, B., Aleman, A., Zanobetti, A., Schwartz, J., Dang, T. N., Dung, D. V., Gillett, N., Haines, A., Mengel, M., Huber, V., and Gasparrini, A. (2021). "The burden of heat-related mortality attributable to recent human-induced climate change". en. In: *Nature Climate Change* 11.6, pp. 492–500.